# ACCURACY ASSESSMENT OF SPLIT-WINDOW AND ENTERPRISE ALGORITHMS FOR LST ESTIMATION FROM VIIRS-NOAA-20

#### Fatima Zahrae Rhziel

Systems and Telecommunications Research Unit, National School for Applied Sciences of Tetouan, University Abdelmalek Essaadi, Remote Sensing, Tetuan, 93000, Morocco fatimazahrae.rhziel @etu.uae.ac.ma

#### Mohammed Lahraoua

Systems and Telecommunications Research Unit, National School for Applied Sciences of Tetouan, University Abdelmalek Essaadi, Remote Sensing, Tetuan, 93000, Morocco m lahraoua@yahoo.fr

## Naoufal Raissouni

Systems and Telecommunications Research Unit, National School for Applied Sciences of Tetouan, University Abdelmalek Essaadi, Remote Sensing, Tetuan, 93000, Morocco naoufal.raissouni.ensa@gmail.com

#### Abstract

Land Surface Temperature (LST) is a key parameter for climate and environmental studies, typically derived from satellite thermal infrared observations. Accurate estimation of LST requires correction for atmospheric absorption and surface emissivity. This study compares the Split-Window Algorithm (SWA) and the Enterprise Algorithm (EA) for LST retrieval from the Visible Infrared Imaging Radiometer Suite (VIIRS) onboard the National Oceanic and Atmospheric Administration (NOAA)-20 satellite. Algorithm coefficients were derived from 135,000 synthetic cases generated with the MODTRAN 4.0 radiative transfer model, using Thermodynamic Initial Guess Retrieval (TIGR-2) atmospheric profiles and emissivity spectra from the Advanced Spaceborne Thermal Emission and Reflection Radiometer (ASTER) library. Sensitivity analyses assessed the impact of sensor noise, emissivity uncertainty, and atmospheric water vapor. Results indicate that emissivity uncertainty dominates retrieval errors, with SWA achieving 1.25–1.64 K and EA 1.80–2.29 K. Validation at the Walpeup and Hay sites in Australia confirmed both methods perform consistently, with SWA slightly more robust under variable conditions.

Keywords: Land Surface Temperature; VIIRS; NOAA-20; Split-Window Algorithm; Enterprise Algorithm.

## 1. Introduction

Land Surface Temperature (LST) is a fundamental parameter in land–atmosphere interactions, reflecting the exchange of energy and heat fluxes between the Earth's surface and the atmosphere [1], [2]. It plays a critical role in a wide range of applications, including evapotranspiration estimation [3], soil moisture monitoring [4], and climatic, hydrological, and ecological studies [5]–[7]. Because of its importance, LST has been routinely derived from thermal infrared (TIR) satellite observations for decades, providing valuable information for global environmental and climate research.

Despite its significance, retrieving accurate LST from satellite measurements remains challenging due to the influence of atmospheric absorption and emission, particularly from water vapor, as well as variations in land surface emissivity [8], [9]. These factors introduce uncertainties that must be corrected to achieve reliable LST estimates. Over the years, several retrieval algorithms have been developed to address these issues [10]–[17]. Among these, the split-window (SW) technique has been the most widely adopted, as it effectively reduces

DOI: 10.21817/indjcse/2025/v16i5/251605001 Vol. 16 No. 5 Sep-Oct 2025

atmospheric distortions by exploiting the difference in brightness temperatures between two adjacent TIR channels. In parallel, the Enterprise Algorithm (EA) has been operationally implemented to provide consistent LST products for NOAA and JPSS missions.

This study evaluates the performance of SWA and EA for LST retrieval from the VIIRS instrument onboard NOAA-20. Using simulations based on MODTRAN 4.0 combined with TIGR atmospheric profiles, along with ground-based validation from two sites in Australia, we aim to quantify algorithm accuracy, assess sensitivity to key uncertainties, and provide insights into their suitability for operational LST estimation.

#### 2. Materials and methods

#### 2.1. Theoretical basis

The retrieval of Land Surface Temperature (LST) from thermal infrared (TIR) satellite measurements is fundamentally based on the Radiative Transfer Equation (RTE). This equation models the total radiance measured at the satellite sensor as the sum of surface emission, the upwelling atmospheric radiance, and the downwelling atmospheric radiance reflected by the Earth's surface and attenuated during transmission through the atmosphere. Under clear sky and local thermodynamic equilibrium conditions, the top of atmosphere radiance measured by a space-borne sensor in a given TIR channel i, at a view zenith angle  $\theta$  can be written as:

$$L_{\text{sensor,i}}(\theta) = \left(\varepsilon_{i} B_{i}(T_{s}) + (1 - \varepsilon_{i}) L_{i}^{\downarrow}\right) \tau_{i}(\theta) + L_{i}^{\uparrow}(\theta) \tag{1}$$

where  $L_{sensor,i}(\theta)$  represents the radiance measured at the sensor in channel i and at a view zenith angle  $\theta$ . The term  $\epsilon_i$  is the surface emissivity for channel i,  $T_s$  is the land surface temperature,  $B_i(T_s)$  denotes the surface radiance calculated using Planck's function,  $\tau_i(\theta)$  is the effective atmospheric transmittance at angle  $\theta$ ,  $L_i^{\downarrow}$  and  $L_i^{\uparrow}(\theta)$  represent the atmospheric downward and upward radiances, respectively.

According to Planck's law,  $B_i(T_s)$  is defined as:

$$B_i(T_s) = \frac{c_1 \lambda_i^{-5}}{\exp\left(\frac{c_2}{\lambda_i T}\right) - 1} \tag{2}$$

where  $c_1=1.19104 \times 10^8 \text{ W} \mu\text{m}^4\text{sr}^1\text{m}^{-2}$  and  $c_2=1.43877 \times 10^8 \mu\text{m}$  K are physical constants, and  $\lambda_i$  is the effective wavelength for channel i, computed as a weighted average of monochromatic wavelengths values using the channel's spectral response function (SRF)  $f_i(\lambda)$ , as follows:

$$\lambda_{i} = \frac{\int_{\lambda_{1,i}}^{\lambda_{2,i}} f_{i}(\lambda) \lambda d\lambda}{\int_{\lambda_{1,i}}^{\lambda_{2,i}} f_{i}(\lambda) d\lambda}$$
(3)

where  $\lambda_{l,i}$  and  $\lambda_{2,i}$  denote the lower and upper wavelength limits of channel i, respectively.

To retrieve LST from Eq. (1), it is crucial to account for and minimize the effects of atmospheric parameters (e.g., downwelling and upwelling radiance, transmittance) and surface emissivity. Several approaches have been developed for this purpose, each relying on different assumptions. Among them, the SWA and the EA are two widely used methods for estimating LST from VIIRS onboard the NOAA-20 satellite, both designed to reduce atmospheric and emissivity influences and ensure accurate LST retrieval.

## 2.2. VIIRS characteristics

The Visible Infrared Imaging Radiometer Suite (VIIRS) is a whiskbroom scanning radiometer carried aboard the Suomi National Polar-orbiting Partnership (S-NPP), NOAA-20, NOAA-21, and future Joint Polar Satellite System (JPSS) series-satellites. It is designed to provide global observations of the land, ocean, atmosphere, and cryosphere by collecting visible and infrared imagery as well as radiometric measurements of surface and cloud properties [18], [19]. VIIRS features 22 spectral bands spanning wavelengths from approximately 0.41 to 12.5 µm, comprising five high-resolution imaging bands (I-bands) and sixteen moderate-resolution bands (M-bands), in addition to a panchromatic Day/Night Band (DNB) for low-light imaging. For LST retrieval, VIIRS primarily uses its two thermal infrared split-window channels: M15 and M16. The M-bands employed for LST retrieval from NOAA-20 are summarized in Table 1.

VIIRS bands	Wavelength (μm)	Bandwidth (µm)	Spatial Resolution (m)
M15	10.763	10.26–11.26	
M16	12.013	11.54–12.49	750

Table 1. The characteristics of VIIRS NOAA-20 M15 and M16 bands.

The spectral response function (SRF) of the two VIIRS TIR bands are shown in Fig. 1.

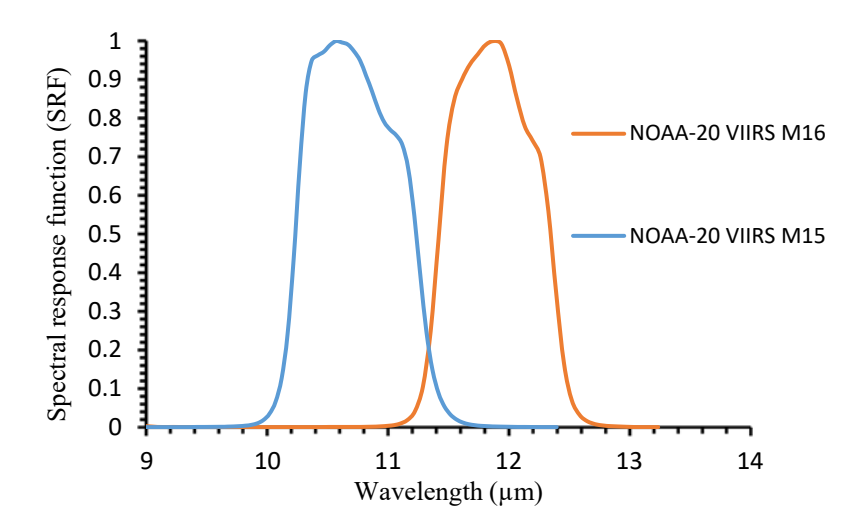


Fig. 1. Spectral response functions of VIIRS NOAA-20 bands M15 and M16.

## 2.3. Split Window Algorithm

The Split-Window Algorithm (SWA) is one of the most widely used techniques for retrieving LST from satellite data. It requires sensors equipped with at least two TIR bands, typically centered around 11  $\mu$ m and 12  $\mu$ m. Originally introduced by McMillin [20] for sea surface temperature retrieval, the method was later adapted for LST estimation from a variety of sensors [21]–[24]. The principle of the SWA relies on the differential absorption between two adjacent TIR channels, which allows partial correction of atmospheric effects, particularly those caused by water vapor.

Over the years, several modifications and parameterizations have been proposed to improve its accuracy, each adapted to specific atmospheric conditions or sensor characteristics. Li et al. [9] provided a comprehensive overview of these approaches, highlighting their theoretical basis and assumptions.

In this study, we employ the SWA developed by Sobrino and Raissouni [15], which incorporates corrections for emissivity and atmospheric water vapor, and is formulated as follows:

$$T_{s} = T_{i} + c_{1}(T_{i} - T_{j}) + c_{2}(T_{i} - T_{j})^{2} + c_{0} + (c_{3} + c_{4}W)(1 - \epsilon) + (c_{5} + c_{6}W)\Delta\epsilon$$
 (4)

where Ts is the land surface temperature (in K), Ti and Tj are the at-sensor brightness temperatures from the VIIRS M15 and M16 bands (in K),  $\varepsilon = (\varepsilon i + \varepsilon j)/2$  and  $\Delta \varepsilon = (\varepsilon i - \varepsilon j)$  are the mean effective emissivity and the emissivity difference between the two bands, respectively; w is the total atmospheric water vapor content (g/cm<sup>2</sup>); and c<sub>0</sub> to c<sub>6</sub> are regression coefficients derived from simulated data.

## 2.4. Enterprise Algorithm

The Enterprise Algorithm (EA) is the operational approach adopted for generating LST from VIIRS data. It is designed to provide a consistent and computationally efficient framework for global LST retrievals within the NOAA processing system. The EA applies a linear regression model that relates top-of-atmosphere brightness temperatures from the VIIRS split-window channels to surface temperature, while incorporating emissivity and emissivity-difference terms to account for land surface radiative properties. According to the Theoretical Basis Document (TBD) for VIIRS LST production, the EA is expressed as [25], [26]:

$$T_s = c_0 + c_1 T_i + c_2 (T_i - T_j) + c_3 \varepsilon + c_4 \varepsilon (T_i - T_j) + c_5 \Delta \varepsilon$$
 (5)

where Ts is the land surface temperature (in K), Ti and Tj are the at-sensor brightness temperatures from the VIIRS M15 and M16 bands (in K),  $\varepsilon$  and  $\Delta\varepsilon$  are the mean effective emissivity and the emissivity difference between the two bands, respectively, as defined previously; and  $c_0$  to  $c_5$  are regression coefficients derived from simulated data, consistent with the SWA formulation.

#### 2.5. Simulation and regression process

The coefficients for the SWA and the EA were derived from simulated data generated using the MODerate spectral resolution atmospheric TRANsmission (MODTRAN 4.0) radiative code. This approach models the relationship between input LST and the resulting top-of-atmosphere (TOA) brightness temperatures, after which regression analysis is performed to obtain the coefficients required for LST retrieval.

Following previous studies [27], [28], we used MODTRAN 4.0 [29] with the VIIRS spectral response functions for bands M15 and M16 to simulate the key atmospheric parameters: transmittance  $(\tau_i)$ , downwelling radiance  $(L_i^{\uparrow})$ , and upwelling radiance  $(L_i^{\uparrow})$ . The simulations were conducted for 54 representative atmospheric profiles extracted from the Thermodynamic Initial Guess Retrieval (TIGR) radiosonde database [30], which contains 2311 global atmospheric profiles spanning a wide range of meteorological conditions with total column water vapor content (WVC) between 0.06 and 8 g/cm². To ensure cloud-free conditions, profiles with relative humidity exceeding 90% in any atmospheric layer were excluded, following Hu et al. [31]. This filtering yielded 1393 clear-sky profiles, from which 54 representative cases were selected. These cover WVC values from 0.15 to 4.65 g/cm² and surface air temperatures ( $T_0$ , bottom-layer temperature) between 230 K and 330 K.

To simulate realistic LST variability, five surface temperature levels were defined relative to To: To-5, To, To+5, To+5, To+10, and To+20. Sensor viewing geometry was accounted for by including five view zenith angles (VZA):  $0^{\circ}$ ,  $10^{\circ}$ ,  $20^{\circ}$ ,  $30^{\circ}$ , and  $40^{\circ}$ . Surface emissivity was derived from the ASTER Spectral Library [32], which provides 100 spectra covering various surface types, including rocks, soils, vegetation, water, snow, and ice. The effective emissivity ( $\epsilon_i$ ) for VIIRS bands was calculated by convolving the spectral emissivity  $\epsilon(\lambda)$  with the VIIRS spectral response function  $f(\lambda)$  [33], according to:

$$\varepsilon_{i} = \frac{\int_{\lambda_{1}}^{\lambda_{2}} f(\lambda)\varepsilon(\lambda)d\lambda}{\int_{\lambda_{1}}^{\lambda_{2}} f(\lambda)d\lambda}$$
 (6)

Altogether, this experimental design produced 135000 simulated cases (54 profiles  $\times$  5 LST levels  $\times$  5 VZAs  $\times$  100 emissivity spectra). MODTRAN outputs were then convolved with the VIIRS M15 and M16 response functions to extract transmittance, downwelling radiance, and upwelling radiance, from which at-sensor brightness temperatures ( $T_i$ ) were computed using Eq. (1) and the inverse Planck function. The simulated brightness temperatures were finally regressed against the input LSTs to derive the coefficients for both the SWA and EA (Eq. (4) and Eq. (5)). Fig. 2 summarizes the methodology for algorithm coefficient development.

# 2.6. Validation sites

Validation of LST retrieval is essential to ensure that satellite-derived estimates meet accuracy requirements. One of the most common approaches is ground-based validation, where remotely sensed LST is compared against in situ measurements. In this study, two homogeneous sites in Australia, Walpeup and Hay, were selected for validation following the description by Prata [34]. At both sites, solid-state temperature transducers were used to provide in situ surface temperature measurements [35]. Further details on the operation and calibration of these instruments are given in [35].

The geolocation and surface characteristics of the sites are summarized in Table 2.

Site	Location (Lat, Lon)	Surface Type
Walpeup, northwest of Melbourne	35°12′S, 142°36′E	Cropland
Hay, NewSouthWales	23°24′S, 145°18′E	Vegetation/soil mixture

Table 2. Geolocation and surface type of the validation sites.

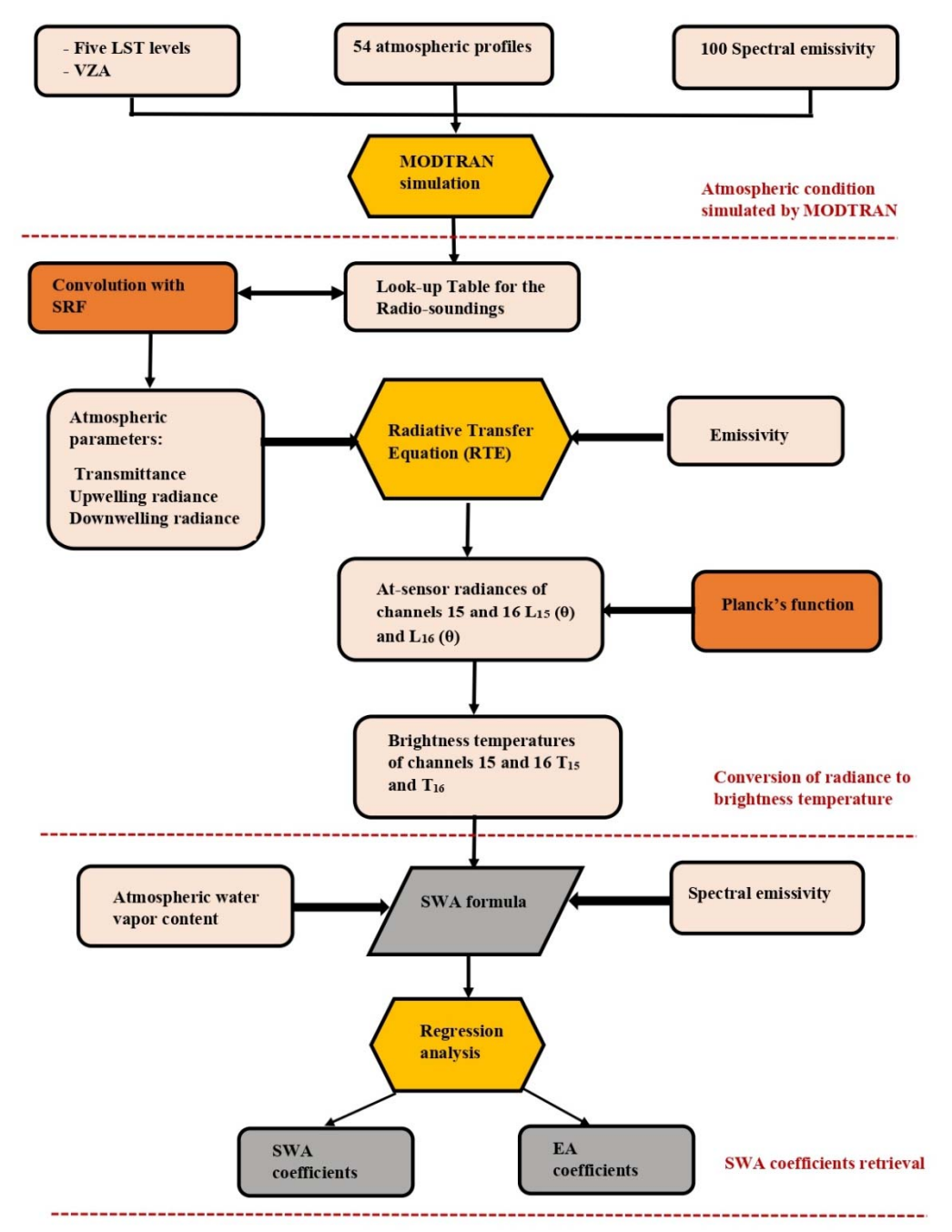


Fig. 2. Workflow for deriving coefficients of the Split-Window Algorithm (SWA) and Enterprise Algorithm (EA).

## 3. Results and discussion

## 3.1. Coefficients of Split-Window and Enterprise algorithms

Table 3 lists the regression coefficients of the SWA and the EA, derived from MODTRAN 4.0 radiative transfer simulations. These coefficients are used for estimating LST from VIIRS NOAA-20 observations.

Method	C0	C1	C2	C3	C4	C5	C6
Split-Window Algorithm	-0.16	1.331	0.234	58.10	-0.57	-112.00	8.84
Enterprise Algorithm	58.22	1.000	2.889	-58.89	0.019	-148.57	_

Table 3. Regression coefficients of the SWA and EA for LST retrieval from VIIRS NOAA-20.

#### 3.2. Sensitivity analysis of the algorithms

To evaluate the robustness of the developed SWA and the EA, a sensitivity analysis was carried out to quantify the influence of major uncertainty sources on the retrieved LST. According to Wan and Dozier [22], three primary error sources were considered: (i) sensor noise (NE $\Delta$ T), (ii) land surface emissivity (LSE), and (iii) atmospheric water vapor content (WVC).

The total error ( $\delta_{Total}$ ) in LST can be expressed as:

$$\delta_{Total}(T_S) = \sqrt{\delta_{alg}^2 + \delta_{NE\Delta T}^2 + \delta_{\varepsilon}^2 + \delta_{W}^2}$$
 (7)

where  $\delta_{alg}$  is the standard deviation associated with the algorithm, and  $\delta_{NE\Delta T}$ ,  $\delta_{\epsilon}$  and  $\delta_{W}$  are the contribution to the total error arising from sensor noise, emissivity and atmospheric water vapor, respectively, These terms are estimated as follows:

$$\delta_{\text{NE}\Delta T} = \sqrt{\left(\frac{\partial T_S}{\partial T_{15}}\right)^2 e^2(T_{15}) + \left(\frac{\partial T_S}{\partial T_{16}}\right)^2 e^2(T_{16})}$$
(8)

$$\delta \varepsilon = \sqrt{\left(\frac{\partial T_S}{\partial \varepsilon}\right)^2 e^2(\varepsilon) + \left(\frac{\partial T_S}{\partial \Delta \varepsilon}\right)^2 e^2(\Delta \varepsilon)}$$
 (9)

$$\delta_{W} = \left(\frac{\partial T_{S}}{\partial W}\right) e(W) \tag{10}$$

where, e(T15) and e(T16) denote the radiometric noise (NE $\Delta$ T) for the VIIRS channels M15 and M16, with values of 0.070 K and 0.072 K, respectively, as reported in the VIIRS LST Algorithm Theoretical Basis Document [25]. The terms e( $\epsilon$ 15) and e( $\epsilon$ 16) denote the emissivity uncertainties, commonly assumed to be 0.01 in most LST estimation studies [36]. To further assess the impact of emissivity uncertainty on LST retrieval, two levels were considered: 0.01 and 0.005 (i.e., e( $\epsilon$ 15) = e( $\epsilon$ 16) = 0.01 and e( $\epsilon$ 15) = e( $\epsilon$ 16) = 0.005). Finally, e(w) denotes the WVC uncertainty, set to 0.5 g/cm² following [37].

For the SWA, all four error components ( $\delta alg$ ,  $\delta_{NE\Delta T}$ ,  $\delta \epsilon$ ,  $\delta_W$ ) contribute to the total uncertainty. In contrast, the EA formulation (Equation 5) does not explicitly include WVC. As a result, the WVC error term is excluded, and only  $\delta alg$ ,  $\delta_{NE\Delta T}$ , and  $\delta \epsilon$  are considered in the total LST error.

Table 4 summarizes the sensitivity analysis results for both algorithms. For each error source, the contribution to LST uncertainty is reported, along with the total propagated error under the two emissivity uncertainty scenarios.

Error source (K)	δalg	δΝΕΔΤ	δε (0.01)	δε (0.005)	δW	δTotal (0.01)	δTotal (0.005)
SWA	1.07	0.20	1.23	0.62	0.02	1.64	1.25
EA	1.60	0.49	1.56	0.67	I	2.29	1.80

Table 4. Error contributions for the Split-Window Algorithm (SWA) and Enterprise Algorithm (EA) in LST retrieval.

The sensitivity analysis results (Table 4) highlights clear differences between the two algorithms. For both SWA and EA, emissivity uncertainty ( $\delta\epsilon$ ) is the dominant error source, particularly at the higher uncertainty level of 0.01, where it contributes over 1 K to the total LST error. When reduced to 0.005, this contribution is nearly halved, highlighting the critical role of accurate emissivity characterization in LST retrieval. Algorithmic uncertainty ( $\delta$ alg) also plays a major role, with a larger effect in the EA (1.60 K) compared to the SWA (1.07 K), which explains the consistently higher total error of the EA. Sensor noise ( $\delta$ <sub>NE $\Delta$ T</sub>) introduces smaller errors, although its effect is more pronounced for EA (0.49 K) than for SWA (0.20 K). For SWA, the additional WVC uncertainty contributes minimally (0.02 K), confirming that WVC errors are not a major limiting factor in this context.

Overall, the total LST ( $\delta_{Total}$ ) error ranges between 1.25–1.64 K for SWA and 1.80–2.29 K for EA. This indicates that the SWA achieves slightly more robust LST retrieval under varying uncertainty conditions, while the EA is more sensitive to algorithmic and sensor noise errors. These results emphasize that while both algorithms perform reasonably well, improvements in emissivity characterization and algorithm calibration are essential to

Fatima Zahrae Rhziel et al / Indian Journal of Computer Science and Engineering (IJCSE)

e-ISSN: 0976-5166 p-ISSN: 2231-3850

further reduce LST retrieval uncertainty. Moreover, the dominance of emissivity as the primary source of error, contrasted with the negligible role of WVC when its uncertainty is constrained, aligns with the results of Chen et al. [38] and Sobrino et al. [39]. This further underscores the importance of precise emissivity characterization in enhancing LST accuracy.

## 3.3. Validation of the algorithms

The accuracy of the retrieved LST from VIIRS NOAA-20 was evaluated by validating the SWA and EA results against in-situ observations at the Walpeup and Hay sites, using the ground truth datasets described in Section 2. Table 5 presents the statistical metrics, including mean bias, standard deviation, and RMSE, which provide a quantitative assessment of the performance and reliability of each algorithm in reproducing ground-based LST measurements.

Site	Method	Bias (K)	Std. Dev. (K)	RMSE (K)
Walaawa	SWA	1.28	1.38	1.88
Walpeup	EA	1.14	1.84	1.84
Hay	SWA	1.07	1.24	1.64
	EA	1.64	1.57	1.57

Table 5. Validation statistics of LST retrieved from VIIRS NOAA-20 using SWA and EA against ground measurements at Walpeup and Hay sites.

Table 5 summarizes the validation results of the retrieved LST from NOAA-20 VIIRS using the SWA and EA against in-situ measurements at the Hay and Walpeup sites. Both algorithms demonstrate satisfactory performance, with biases ranging between 1.07 K and 1.64 K, indicating reasonable agreement with ground observations.

At Walpeup, the SWA achieved a bias of 1.28 K and RMSE of 1.88 K, while the EA yielded a slightly lower bias of 1.14 K and a comparable RMSE of 1.84 K. This suggests that both algorithms perform similarly, with EA reducing systematic error and SWA providing marginally better consistency (standard deviation of 1.38 K vs. 1.84 K). At Hay, the SWA demonstrated superior performance relative to EA, achieving lower bias (1.07 K vs. 1.64 K), lower standard deviation (1.24 K vs. 1.57 K), and a slightly higher RMSE (1.64 K vs. 1.57 K). Despite the small difference in RMSE, the overall stability and accuracy of SWA at this site indicate its advantage under local conditions.

These findings highlight that algorithm performance may vary depending on site-specific characteristics, such as land surface properties and atmospheric variability. In general, both SWA and EA are reliable for LST retrieval, with SWA showing a relative advantage at Hay and EA performing marginally better at Walpeup.

#### 4. Conclusion

This study presents a systematic comparison of the SWA and the EA for retrieving LST from VIIRS onboard NOAA-20. Through extensive MODTRAN simulations and validation against in-situ measurements at Walpeup and Hay, both algorithms demonstrated reliable performance, with biases typically below 1.6 K and RMSE values under 2 K. Sensitivity analysis revealed that emissivity uncertainty is the primary contributor to retrieval errors, while atmospheric water vapor has a minor effect when constrained. The SWA showed slightly higher robustness and lower total uncertainty, highlighting its advantage for operational LST retrieval under varying surface and atmospheric conditions. Overall, these findings confirm that SWA provides a dependable alternative to EA for accurate LST estimation from NOAA-20 data, with potential benefits for climate studies, environmental monitoring, and hydrological applications.

## **Conflict of Interest**

The authors have no conflicts of interest to declare.

#### References

- [1] P. Dash, F. M. Göttsche, F. S. Olesen, and H. Fischer, "Land surface temperature and emissivity estimation from passive sensor data: Theory and practice-current trends," *Int. J. Remote Sens.*, vol. 23, no. 13, pp. 2563–2594, Jul. 2002, doi: 10.1080/01431160110115041;PAGE:STRING:ARTICLE/CHAPTER.
- [2] M. C. Anderson, J. M. Norman, W. P. Kustas, R. Houborg, P. J. Starks, and N. Agam, "A thermal-based remote sensing technique for routine mapping of land-surface carbon, water and energy fluxes from field to regional scales," *Remote Sens. Environ.*, vol. 112, no. 12, pp. 4227–4241, Dec. 2008, doi: 10.1016/J.RSE.2008.07.009.
- [3] G. B. Senay et al., "Long-Term (1986–2015) Crop Water Use Characterization over the Upper Rio Grande Basin of United States

- and Mexico Using Landsat-Based Evapotranspiration," *Remote Sens. 2019, Vol. 11, Page 1587*, vol. 11, no. 13, p. 1587, Jul. 2019, doi: 10.3390/RS11131587.
- [4] J. Sun, G. D. Salvucci, and D. Entekhabi, "Estimates of evapotranspiration from MODIS and AMSR-E land surface temperature and moisture over the Southern Great Plains," *Remote Sens. Environ.*, vol. 127, pp. 44–59, Dec. 2012, doi: 10.1016/J.RSE.2012.08.020.
- [5] B. Candy, R. W. Saunders, D. Ghent, and C. E. Bulgin, "The Impact of Satellite-Derived Land Surface Temperatures on Numerical Weather Prediction Analyses and Forecasts," *J. Geophys. Res. Atmos.*, vol. 122, no. 18, pp. 9783–9802, Sep. 2017, doi: 10.1002/2016JD026417;CTYPE:STRING:JOURNAL.
- [6] M. Cai, C. Ren, Y. Xu, K. K. L. Lau, and R. Wang, "Investigating the relationship between local climate zone and land surface temperature using an improved WUDAPT methodology – A case study of Yangtze River Delta, China," *Urban Clim.*, vol. 24, pp. 485–502, Jun. 2018, doi: 10.1016/J.UCLIM.2017.05.010.
- [7] B. Bechtel, Z.-L. Li, J. A. Sobrino, X. Song, J. Kellndorfer, and P. S. Thenkabail, "A New Global Climatology of Annual Land Surface Temperature," *Remote Sens. 2015, Vol. 7, Pages 2850-2870*, vol. 7, no. 3, pp. 2850–2870, Mar. 2015, doi: 10.3390/RS70302850.
- [8] A. J. Prata, C. V. Casellescoll, J. A. Sobrino, and C. Ottle, "Thermal remote sensing of land surface temperature from satellites: current status and future prospects," *Remote Sens. Rev.*, vol. 12, no. 3–4, pp. 175–224, 1995, doi: 10.1080/02757259509532285.
- [9] Z. L. Li *et al.*, "Satellite-derived land surface temperature: Current status and perspectives," *Remote Sens. Environ.*, vol. 131, pp. 14–37, Apr. 2013, doi: 10.1016/J.RSE.2012.12.008.
- [10] F. Becker and Z. L. Li, "Towards a local split window method over land surfaces," *Remote Sens.*, vol. 11, no. 3, pp. 369–393, 1990, doi: 10.1080/01431169008955028.
- [11] J. C. Jiménez-Munoz and J. A. Sobrino, "A generalized single-channel method for retrieving land surface temperature from remote sensing data," *J. Geophys. Res. Atmos.*, vol. 108, no. 22, 2003, doi: 10.1029/2003jd003480.
- [12] J. C. Price, "Land surface temperature measurements from the split window channels of the NOAA 7 Advanced Very High Resolution Radiometer," *J. Geophys. Res. Atmos.*, vol. 89, no. D5, pp. 7231–7237, Aug. 1984, doi: 10.1029/JD089ID05P07231.
- [13] J. A. Sobrino, J. C. Jiménez-Muñoz, and L. Paolini, "Land surface temperature retrieval from LANDSAT TM 5," *Remote Sens. Environ.*, vol. 90, no. 4, pp. 434–440, 2004, doi: 10.1016/j.rse.2004.02.003.
- [14] B. Tang, Y. Bi, Z. A. Li, and J. Xia, "Generalized split-window algorithm for estimate of land surface temperature from Chinese geostationary FengYun meteorological satellite (FY-2C) data," *Sensors*, vol. 8, no. 2, pp. 933–951, 2008, doi: 10.3390/s8020933.
- [15] J. A. Sobrino and N. Raissouni, "Toward remote sensing methods for land cover dynamic monitoring: Application to Morocco," Int. J. Remote Sens., vol. 21, no. 2, pp. 353–366, 2000, doi: 10.1080/014311600210876.
- [16] C. Coll and V. Caselles, "A split-window algorithm for land surface temperature from advanced very high resolution radiometer data: Validation and algorithm comparison," *J. Geophys. Res. Atmos.*, vol. 102, no. 14, pp. 16697–16713, 1997, doi: 10.1029/97jd00929.
- [17] A. Gillespie, S. Rokugawa, T. Matsunaga, J. Steven Cothern, S. Hook, and A. B. Kahle, "A temperature and emissivity separation algorithm for advanced spaceborne thermal emission and reflection radiometer (ASTER) images," *IEEE Trans. Geosci. Remote Sens.*, vol. 36, no. 4, pp. 1113–1126, 1998, doi: 10.1109/36.700995.
- [18] C. Cao, F. De Luccia, ... X. X.-I. T. on, and undefined 2013, "Early on-orbit performance of the visible infrared imaging radiometer suite onboard the Suomi National Polar-Orbiting Partnership (S-NPP) satellite," *ieeexplore.ieee.orgC Cao, FJ Luccia, X Xiong, R Wolfe, F WengIEEE Trans. Geosci. Remote Sensing, 2013\*ieeexplore.ieee.org*, Accessed: Aug. 31, 2025. [Online]. Available: https://ieeexplore.ieee.org/abstract/document/6522157/
- [19] G. Hulley, N. Malakar, ... T. I.-I. J. of, and undefined 2017, "NASA's MODIS and VIIRS land surface temperature and emissivity products: A long-term and consistent earth system data record," *ieeexplore.ieee.org*, Accessed: Aug. 31, 2025. [Online]. Available: https://ieeexplore.ieee.org/abstract/document/8241381/
- [20] L. M. McMillin, "Estimation of sea surface temperatures from two infrared window measurements with different absorption," J. Geophys. Res., vol. 80, no. 36, pp. 5113–5117, Dec. 1975, doi: 10.1029/JC080I036P05113.
- [21] J. A. Sobrino, Z. L. Li, M. P. Stoll, and F. Becker, "Improvements in the Split-Window Technique for Land Surface Temperature Determination," *IEEE Trans. Geosci. Remote Sens.*, vol. 32, no. 2, pp. 243–253, 1994, doi: 10.1109/36.295038.
- [22] J. Wan, Z. Dozier, "A generalized split-window algorithm for retrieving land-surface temperature from space," *IEEE Trans. Geosci. Remote sensing, 1996-ieeexplore.ieee.org*, vol. 34, no. 4, 1996, Accessed: Jun. 17, 2025. [Online]. Available: https://ieeexplore.ieee.org/abstract/document/508406/
- [23] Y. Yu et al., "Validation of GOES-R satellite land surface temperature algorithm using SURFRAD ground measurements and statistical estimates of error properties," *IEEE Trans. Geosci. Remote Sens.*, vol. 50, no. 3, pp. 704–713, Mar. 2012, doi: 10.1109/TGRS.2011.2162338.
- [24] Y. Yu et al., "Developing algorithm for operational GOES-R land surface temperature product," *IEEE Trans. Geosci. Remote Sens.*, vol. 47, no. 3, pp. 936–951, Mar. 2009, doi: 10.1109/TGRS.2008.2006180.
- [25] W. H. Yu Yunyue, Liu Yuling, Yu Peng, "Enterprise Algorithm Theoretical Basis Document For VIIRS Land Surface Temperature Production Compiled by the SPSRB Common Standards Working Group," 2021.
- [26] M. M. XiangChen and C. C. Jie, "Estimating land surface temperature from Landsat-8 data using the NOAA JPSS Enterprise algorithm.," 2019, doi: 10.5555/20193294658.
- [27] Y. Yu, J. L. Privette, and A. C. Pinheiro, "Analysis of the NPOESS VIIRS land surface temperature algorithm using MODIS data," *IEEE Trans. Geosci. Remote Sens.*, vol. 43, no. 10, pp. 2340–2349, 2005, doi: 10.1109/TGRS.2005.856114.
- [28] H. Ouaidrari, S. Goward, ... K. C.-R. S. of, and undefined 2002, "Land surface temperature estimation from AVHRR thermal infrared measurements: An assessment for the AVHRR Land Pathfinder II data set," ElsevierH Ouaidrari, SN Goward, KP Czajkowski, JA Sobrino, E VermoteRemote Sens. Environ. 2002 Elsevier, Accessed: Aug. 31, 2025. [Online]. Available: https://www.sciencedirect.com/science/article/pii/S0034425701003388
- [29] A. Berk et al., "MODTRAN4 Version 3 Revision 1 USER' S MANUAL Space Vehicles Directorate AIR FORCE MATERIEL COMMAND," ReVision, no. February, 2003.
- [30] A. Chedin, N. A. Scott, C. Wahiche, and P. Moulinier, "The Improved Initialization Inversion Method: A High Resolution Physical Method for Temperature Retrievals from Satellites of the TIROS-N Series," *J. Appl. Meteorol. Climatol.*, vol. 24, no. 2, pp. 128–143, Feb. 1985, doi: 10.1175/1520-0450(1985)024.
- T. Hu et al., "Estimation of Surface Upward Longwave Radiation Using a Direct Physical Algorithm," *IEEE Trans. Geosci. Remote Sens.*, vol. 55, no. 8, pp. 4412–4426, Aug. 2017, doi: 10.1109/TGRS.2017.2692261.
- [32] A. M. Baldridge, S. J. Hook, C. I. Grove, and G. Rivera, "Remote Sensing of Environment The ASTER spectral library version 2 . 0," *Remote Sens. Environ.*, vol. 113, no. 4, pp. 711–715, 2009, doi: 10.1016/j.rse.2008.11.007.
- [33] B. Tang, H. Wu, and C. Li, "Estimation of broadband surface emissivity from narrowband emissivities," opg.optica.orgBH Tang,

- H Wu, C Li, ZL LiOptics express, 2010•opg.optica.org, 2010, Accessed: Jun. 17, 2025. [Online]. Available: https://opg.optica.org/abstract.cfm?uri=oe-19-1-185
- [34] A. J. Prata, "Land surface temperatures derived from the advanced very high resolution radiometer and the along-track scanning radiometer 2. Experimental results and validation of AVHRR algorithms results are considered to represent the at a scale of 1-10 km (• IøC ," vol. 99, pp. 25–58, 1994.
- [35] A. J. Prata, "Land surface temperatures derived from the advanced very high resolution radiometer and the along-track scanning radiometer 2. Experimental results and validation of AVHRR algorithms," *J. Geophys. Res.*, vol. 99, no. D6, 1994, doi: 10.1029/94jd00409.
- [36] V. Caselles, E. Valor, C. Coll, and E. Rubio, "Thermal band selection for the PRISM instrument: 1. Analysis of emissivity-temperature separation algorithms," Wiley Online Libr. Caselles, E Valor, C Coll, E Rubio Journal Geophys. Res. Atmos. 1997-Wiley Online Libr., vol. 102, no. 10, pp. 11145–11164, May 1997, doi: 10.1029/97JD00344.
- [37] S. Vey, R. Dietrich, A. Rülke, M. Fritsche, P. Steigenberger, and M. Rothacher, "Validation of Precipitable Water Vapor within the NCEP/DOE Reanalysis Using Global GPS Observations from One Decade," *J. Clim.*, vol. 23, no. 7, pp. 1675–1695, Apr. 2010, doi: 10.1175/2009JCLI2787.1.
- [38] Y. Chen, S. B. Duan, H. Ren, J. Labed, and Z. L. Li, "Algorithm Development for Land Surface Temperature Retrieval: Application to Chinese Gaofen-5 Data," *Remote Sens. 2017, Vol. 9, Page 161*, vol. 9, no. 2, p. 161, Feb. 2017, doi: 10.3390/RS9020161.
- [39] J. A. Sobrino, J. C. Jiménez-Munoz, J. El-Kharraz, M. Gómez, M. Romaguera, and G. Sòria, "Single-channel and two-channel methods for land surface temperature retrieval from DAIS data and its application to the Barrax site," *Int. J. Remote Sens.*, vol. 25, no. 1, pp. 215–230, Jan. 2004, doi: 10.1080/0143116031000115210.

## **Authors Profile**



Rhziel Fatima Zahrae is a Ph.D. candidate in telecommunications and remote sensing at the Remote Sensing, Systems, and Telecommunications (RST) research unit at the National School of Applied Sciences, University of Abdelmalek Essaadi, Tetouan, Morocco. She obtained her master's degree in signal processing and machine learning from the National School of Applied Sciences (ENSA), Tetouan, Morocco, in 2019, and her bachelor's degree in physics from Sidi Mohammed Ben Abdellah University, Fes, Morocco, in 2017. Her research focuses on remote sensing, land surface temperature (LST), and thermal infrared sensors. She is particularly interested in developing retrieval algorithms for LST estimation and leveraging remote sensing data and techniques to monitor land surface temperature and assess the performance of thermal infrared sensors.



**Mohammed Lahraoua** received the Ph.D. degree in Telecommunications and Informatics, in 2011 from University Abdelmalek Essaadi (UAE). degree in Bioinformatics from University Abdelmalek Essaadi (UAE), Tetuan, Morocco, in 1992 and 2004 respectively. Currently, he is a member of Remote Sensing, systems and telecommunications (RST) research group. His present investigations include remote sensing algorithms, thermal infrared satellite imagery of the earth's surface and the development of remote sensing methods for land cove dynamic monitoring and Grid computing.



Naoufal Raissouni received the M.S., and Ph.D. degrees in physics from the University of Valencia, Spain, in 1997, and 1999, respectively. He has been a Professor of physics and remote sensing at the National Engineering School for Applied Sciences of the University Abdelmalek Essaadi (UAE) of Tetuan, since 2003. He is also heading the Innovation & Telecoms Engineering research group at the UAE, responsible of the Remote Sensing & Mobile GIS unit. His research interests include atmospheric correction in visible and infrared domains, the retrieval of emissivity and surface temperature from satellite image, huge remote sensing computations, Mobile GIS, Adhoc networks and the development of remote sensing methods for land cover dynamic monitoring.